Citation: Applied Optics Vol. 46, Issue 22, pp. 4871- 4878 (2007)

https://doi.org/10.1364/AO.46.004871

VUV coatings of Al protected with MgF_2 prepared both by ion-beam-sputtering and by evaporation

Mónica Fernández-Perea, Juan I. Larruquert, José A. Aznárez, Alicia Pons, José A. Méndez

GOLD, Instituto de Física Aplicada-Consejo Superior de Investigaciones Científicas, C/ Serrano 144, 28006 Madrid, Spain; phone: 34 91 561 8806; fax: 34 91 411 7651, email of J. I. Larruquert: larruquert@ifa.cetef.csic.es

Ion-beam-sputtering (IBS) and evaporation are the two deposition techniques that have been used to deposit coatings of Al protected with MgF_2 with high reflectance in the vacuum ultraviolet down to 115 nm. Evaporation deposited (ED) Al protected with IBS MgF_2 resulted in a larger (smaller) reflectance below (above) 125 nm than the well-known all-evaporated coatings. A similar comparison is obtained when the Al film is deposited by IBS instead of evaporation. The lower reflectance of the coatings protected with IBS vs. ED MgF_2 above 125 nm is due to the larger absorption of the former. Both nonprotected IBS Al, as well as IBS Al protected with ED MgF_2, resulted in a band of reflectance loss that was peaked at 127 and 157 nm, respectively, which was attributed to the excitation of surface plasmons due to the enhancement of surface roughness with large spatial wavevectors in the sputter deposition. This reflectance loss for IBS Al protected with MgF_2 is small at the short (λ~120 nm) and long (λ>350 nm) wavelengths investigated. IBS Al protected with ED MgF_2 is then a promising coating for these two spectral regions. Coatings protected with IBS MgF_2 resulted in a reflectance as large as

coatings protected with ED MgF_2 at wavelengths longer than 550 nm, whereas the former had a lower reflectance below this wavelength.

OCIS Codes: 260.7210 Ultraviolet, far; 260.7200 Ultraviolet, extreme; 230.4170 Multilayers; 120.5700 Reflection; 310.6860 Thin films: optical properties; 350.6090 Space Optics

1. INTRODUCTION

The large reflectance of pure Al films in the vacuum UV (VUV) down to 83 nm has been known for decades[1,2,3]. This high reflectance was determined once in-situ reflectance measurements could be performed to avoid the growth of the thin, self-protective, native oxide film, which cancels Al high reflectance at wavelengths shorter than ~200 nm[4]. Protective coatings for Al based on MgF_2 and LiF are known also from those pioneering times[5,6,7]. These coatings preserve Al high reflectance longward of their respective cutoffs. Even though LiF has the shortest cutoff, at 105 nm, and it provides protection for Al mirrors with large reflectance down to that wavelength, MgF_2, with the cutoff at 115 nm, has been more widely used because of its stability, versus the hygroscopic behaviour of LiF. Hence, an Al film protected with a thin MgF_2 film, both materials deposited by evaporation, has been the standard reflective coating for the VUV above 115 nm for over four decades. In such a long time, only the implementation of cleaner vacuum systems has resulted in a limited improvement of this coating, with some increase in reflectance. Recently, the effect of exposing these coatings to controlled doses of air and pure gases onto the VUV reflectance has been measured[8].

Sputtering technology has undergone a dramatic development in the last decades, and coatings prepared with the different sputtering techniques have surpassed in some cases the performance of optical coatings traditionally prepared by means of evaporation techniques. As an example, some VUV and extreme UV coatings of best performance have been prepared by sputtering techniques, such as single layers of SiC[9,10] and B_4C[11].

However, both Al and MgF_2 present difficulties to be deposited by sputtering techniques. Al films need to grow without the incorporation of O_2 and water vapour, and they have to be protected before accumulating an exposure of few Langmuirs (1 Langmuir=10^{-6} torr× s, 1 torr=75 Pa) to avoid a significant reflectance decay[12,13]. Generally, films deposited by sputtering techniques often grow at rates of ~0.1 nm/s and at an ambient pressure of 10^{-2}-1 Pa of a rare gas, whereas Al films deposited by evaporation may grow at a rate typically higher by a factor of 10 to ~300 at an ambient pressure ranging from 10^{-5} to 10^{-8} Pa for high vacuum to ultra high vacuum (UHV) systems. Even though the partial pressure of oxidizing species in a sputtering process will be several orders of magnitude lower than the operating pressure, reaching a pressure of oxidizing gases as low as in an UHV evaporator involves some extra difficulty.

In spite of these difficulties, Kiyota et al. [14] grew Al films by sputtering techniques with a negligible content of oxygen, although special care was taken, such as the discharge cleaning of the chamber after bakeout, the use of purified Ar gas to reach a water content lower than 50 ppb, and a high deposition rate of 3.7 nm/s, a value closer to evaporation than to sputtering standards. Kortright[15] succeeded in preparing Al/Nb multilayers by magnetron sputtering without any special care, and no signal of oxygen was detected through RBS spectroscopy; the multilayer extreme UV reflectance was roughly half of the expected value, but the lack of coincidence was explained in terms not related to impurities.

Regarding MgF_2, this material as well as other fluorides has a proclivity for growing with a deficiency in fluorine when deposited by sputtering techniques. Depending on

the deposition system, widely varying values of the F-to-Mg ratio have been obtained, such as ~1[16] , ~1.7[17] and 1.98[18]. This deficiency results in an absorption increase[18], which is a drawback for the use of sputtering techniques to deposit MgF_2 coatings for the VUV.

In spite of the increase in VUV absorption of MgF_2 sputtered films compared to films deposited by evaporation, Al films deposited by evaporation and protected with two successive thin films of MgF_2, the first one deposited by evaporation and the second one by ion-beam-sputtering (IBS), which will be referred to as hybrid coatings, have been prepared with a larger reflectance below 125 nm than standard Al/MgF_2 coatings, all deposited by evaporation[19]. However, IBS deposited MgF_2 was found to have a larger extinction coefficient than evaporation deposited (ED) MgF_2 at wavelengths longer than 125 nm, which was responsible for a lower reflectance of the Al film coated with a hybrid MgF_2 protection in this range.

This paper explores the possibilities of using IBS techniques and combinations of IBS and evaporation techniques for the deposition of Al/MgF_2 coatings for the VUV. No special procedure was implemented in order to avoid Al oxidation upon sputtering deposition, except that the chamber was baked. In Section 2 we describe the experimental techniques used in this research, which include IBS and evaporation deposition techniques, and VUV, near UV (NUV) and visible reflectometry. Section 3 presents our experimental data on the reflectance of pure Al films and of Al/MgF_2 coatings in which the two deposition techniques were used both for Al and for MgF_2, and it discusses the differences among the coatings and their possibilities of practical applications.

2. EXPERIMENTAL TECHNIQUES

The main experimental system used in this work consists of two UHV coating systems connected in vacuum to an UHV VUV reflectometer. The reflectometer-deposition system has been described elsewhere[20, 21]. In this equipment both single-layer and multilayer coatings can be prepared both by evaporation and by IBS deposition techniques, and the freshly coated samples can be transferred to the reflectometry chamber without breaking vacuum, where in situ VUV transmittance and reflectance measurements can be performed.

Each of the two connected deposition chambers is specialized in a deposition method, i.e., evaporation or sputtering. The evaporation chamber was evacuated by means of an ion pump along with a Ti sublimation pump, and after baking it up to ~470 K, the base pressure was ~10^{-8} Pa. The sputtering chamber was evacuated with a turbomolecular pump backed with a dry pump, which after a similar bakeout reached a base pressure of ~10^{-7} Pa. Evaporation of 99.999% purity Al was performed from tungsten straight multistranded filaments. Random cuts of UV-grade MgF_2 from Saint Gobain were used to evaporate from molybdenum boats. Sputter coatings were performed by using a 76.2-mm diameter, 99.999% purity Al target and a 97-mm diameter, 99.99% purity MgF_2 target. The respective deposition rates of Al and MgF_2 were ~2.5 and 1.5 nm/s for ED films and 0.18 and 0.08 nm/s for IBS coatings. Film thickness was monitored with a quartz crystal oscillator. These thickness measurements were calibrated through Tolansky interferometry, i.e., through multiple-beam interference fringes in a wedge between two highly reflective surfaces[22].

The sputtering chamber is provided with a rotatable target holder that hosts up to four different targets. A 3-cm, hollow cathode ion source fed with Ar gas extracts atoms from the target, that reach the substrate placed at a distance of 150 mm. A flow of 3.8 sccm of Ar through the ion source and an additional Ar flow of 3.8 sccm through the hollow-cathode neutralizer resulted in a total pressure during sputtering of $\sim 5\times10^{-2}$ Pa. Water was used to cool down the targets. Ion energy and total ion current were set at 1,100 eV and ~45 mA, respectively. The substrates were 50.8x50.8x3-mm^3 pieces of float glass that had been later polished. The substrates were not either heated or cooled down during deposition.

Reflectance measurements in the VUV were performed in situ on samples at room temperature. Reflectance measurements in the near UV to near IR were performed ex situ with a Perkin-Elmer Lambda9 spectrophotometer using the specular reflectance accessory working in V-W configuration.

3. RESULTS AND DISCUSSION

A. Pure Al film

Fig. 1 plots the VUV reflectance of a fresh, ~60-nm thick IBS-Al film. The reflectance measured for a fresh ED Al film, and the reflectance calculated for a smooth, opaque Al film are also plotted for comparison purposes. The optical constants of Al are those of Shiles et. al.[23] in the compilation by Palik[24], that were updated with those of Larruquert et al.[25,26]. Both films were deposited in UHV conditions and the reflectance was measured within a few hours from deposition, before it was affected by oxidation.

The reflectance of the IBS film approaches that of the ED Al film both at short and long wavelengths. This datum is helpful to estimate the content of contaminants in the IBS film. The ED-to-IBS ratio of deposition rates was ~14, and the partial pressure of oxidizing species in the residual atmosphere, which was measured with a residual gas analyzer, was ~30 times larger for the IBS film; therefore it is relevant to wonder whether the IBS film may be affected by oxidation. Hass and Waylonis[27] measured the influence of the deposition speed and chamber pressure onto the reflectance of ED Al films; at a total pressure of ~2×10^{-3} Pa, a deposition rate of 10 nm/s resulted in no apparent reflectance decrease at 220 nm with respect to a pure Al film, but a deposition rate of ~0.5 nm/s at the same pressure resulted in a reflectance loss of ~15% at this wavelength. Hence, a top acceptable limit for the ratio of pressure to deposition rate can be roughly established at ~2×10^{-4} Pa·s/nm at 220 nm, although this top ratio may be smaller at the short wavelengths of the current research. The partial pressure of oxidizing species in the sputtering chamber during a sputter deposition was ~5×10^{-7} Pa, which for a 0.18 nm/s Al deposition rate results in a ratio of ~3×10^{-6} Pa·s/nm, which is almost two orders of magnitude below the above rough limit. From the above, no significant oxygen content is expected in the IBS Al film. Once the film had been deposited, the total exposure of the film during the transfer to the reflectometer and the reflectance measurements is estimated to be ~0.4 Langmuir, which is expected to provide a negligible reflectance decay[13,28]. Other than oxygen, a certain amount of Ar ions may have been buried in the growing Al film. The reflectance of the IBS film at the short wavelength range, the most sensitive to the presence of contaminants, is not much smaller than the one of an ED film, which suggests that the proportion of any contaminants must be small.

The reflectance in the central part of the spectrum displayed in Fig. 1 is clearly lower for the IBS film. This lower reflectance is attributed to surface plasmon excitation in a free-electron metal such as Al. Surface plasmons are evanescent electromagnetic waves that propagate along the surface of the metal. When radiation impinges onto the metallic surface from vacuum, surface plasmons cannot couple directly to the electromagnetic wave when the metallic surface is perfectly smooth since the surface plasmon oscillation lies entirely in the non-radiative region; however, surface plasmons can be excited when surface roughness components with a spatial wavevector larger than ω/c are present, where ω is the radiation frequency and c is the speed of light. In contrast, surface roughness components with a spatial wavevector smaller than ω/c are involved in the scattering of light. The light scattered in a rough surface results in a reflectance loss that monotonously decreases when radiation wavelength increases, for a given roughness distribution. In contrast, surface plasmon excitation results in a reflectance loss in a band peaked at:

$$\lambda_{sp} = \lambda_p \sqrt{1+\varepsilon} \qquad (1)$$

when the free electron has zero damping[29]; ε is the dielectric constant of the medium from which radiation impinges on the free electron metal, which is unity for vacuum; λ_p is the volume plasmon wavelength of the free electron metal, which is 83 nm for Al, and λ_{sp} is called the surface plasmon wavelength, which is ~117 nm for the Al/vacuum interface. Real metals do have some damping, which results in the broadening of the reflectance loss band and in a certain shift of the peak towards longer wavelengths[29].

The difference between the reflectance of the IBS film and that of the smooth Al film has been investigated here to find out whether it can be explained in terms of surface plasmon excitation. The dependence of reflectance on surface roughness was evaluated

using the expressions obtained by Croce[30], in the generalization and notation given by Larruquert et al.[25]. Croce's theory is general in the sense that it takes into account any refractive indices, any incidence angle, and any radiation polarization, and it involves roughness wavevectors both larger and smaller than that of radiation. This theory is a second order perturbation expansion, and it is limited to describe irregularities with average height much smaller than wavelength, which is satisfied here. The paper by Kretschmann and Kröger[29] has been more widely used and cited in literature; however, Croce's paper, with the generalization given in Ref. 25, is more general since it includes any incidence angle, whereas Ref. 29 only applies for normal incidence. The amplitude reflectance and transmittance of a rough surface is obtained with the following expressions:

$$\left.\begin{aligned} r &= r_0\left[1 + A\int d^2\vec{k}\,g(\vec{k})B\right] \\ t &= t_0\left[1 + A'\int d^2\vec{k}\,g(\vec{k})B'\right] \end{aligned}\right\} \qquad (2)$$

where r_0 and t_0 are the Fresnel coefficients of the smooth interface, r and t are the modified coefficients encompassing roughness effects, $d^2\vec{k}$ represents a spatial wavevector element, $g(\vec{k})$ represents the power spectral density of the roughness distribution, and A, A', B, B' are functions of the refractive indices of the media, of wavelength, of radiation polarization and of the incidence angle; these parameters are described in Refs. 30 and 25. The roughness distribution of the Al film, mainly the high spatial frequency components, will be modified with the natural growth of aluminum oxide when the nonprotected Al film is extracted from vacuum. Hence the Al roughness distribution would have to be measured in UHV; unfortunately a technique to measure this in situ was not available. Instead, information of this roughness distribution was obtained from the analysis of the measured reflectance. In this analysis, two different functions, Gaussian and Lorentzian, were considered for the power spectral density. For

simplicity, the power spectral density was assumed to depend only on the modulus of the spatial wavevector and not on its direction. Gaussian functions resulted in a better fitting to the experimental data. The Gaussian power spectral density function is expressed by:

$$g(k) = \pi\sigma^2 T^2 \exp\left(-\frac{k^2 T^2}{4}\right) \qquad (3)$$

where the two free parameters are σ, the root-mean-square roughness, and T, the autocorrelation length. k stands for the spatial wavevector. σ represents the average height of the roughness referred to an average plane; T is related to the average width of the irregularities. The two parameters were calculated through a nonlinear least-squares fitting of the experimental reflectance using Croce's model assuming a Gaussian roughness power spectral density. Fig. 2 displays the reflectance calculated with the fitting parameters σ=3.55 nm, and T=35.4 nm. The current value of T, smaller than the radiation wavelength, confirms that the effective width of the irregularities corresponds to spatial wavevectors that are larger than ω/c, which are responsible for surface plasmon excitation.

From the above we conclude that Al films deposited by IBS grow with an increased short-range roughness. The long-range irregularities for IBS Al might be either similar or slightly larger than for the film deposited by evaporation, according to the small reflectance difference in Fig. 1 at the short wavelengths. However, a slight oxidation and/or Ar inclusion might also be responsible for this small reflectance difference.

B. Al film protected with MgF_2

Fig. 3 plots the reflectance of all combinations of Al protected with MgF_2 deposited by IBS and evaporation. MgF_2 thickness was set at 25 nm in order to obtain the largest possible reflectance at 120 nm. Two regions can be recognized in the figures. At wavelengths of 132 nm and shorter, the reflectance difference of all coatings is relatively small, whereas this difference is largely increased at longer wavelengths. At the short wavelength limit of 120 nm, the IBS-MgF_2 protective coatings result in a slightly larger reflectance than the standard ED MgF_2 both for ED as well as for IBS Al, which is in the line of the results obtained by Larruquert and Keski-Kuha for hybrid coatings[19]. In Ref. 19 Al could not be exclusively protected with IBS MgF_2 because evaporation and sputtering were performed in two nonconnected chambers; hence, the authors protected the Al film with a 7 to 10-nm thick MgF_2 film deposited by evaporation, which gave enough protection for a quick, in-air transfer to the sputtering chamber, where the rest of the protective coating up to a total of ~25 nm was deposited by IBS.

We also obtained that the reflectance at wavelengths of 149.4 and above was much larger for the all-evaporated coating than for the ED Al film protected with IBS MgF_2 film. Qualitatively, this also agrees with the result for the hybrid coatings of Ref. 19, but the reflectance of the latter coatings at these long wavelengths was larger than for the current ED Al film protected with IBS MgF_2; however, the wavelengths at which measurements were performed in the two papers are not coincident, which complicates the comparison. In Ref. 19, the reflectance decrease at wavelengths longer than ~125 nm for the hybrid coatings compared to the standard all-evaporated coatings was attributed to a larger absorption of IBS MgF_2 compared to ED MgF_2. In the current

samples protected with IBS MgF_2 the larger reflectance loss at these same wavelengths compared to the hybrid samples is due to the larger absorption of a full 25-nm-thick IBS MgF_2 film compared to Ref. 19, where about one third of the MgF_2 coating was deposited by evaporation.

In Fig. 3, if we compare coatings of ED Al and IBS Al, both protected with ED MgF_2, the former has a larger reflectance in the whole spectrum, although this difference is relatively small at wavelengths shorter than or equal to 132 nm, and the difference increases at longer wavelengths. It will be shown in the following that this result is in agreement with the result shown on sub-section 3.A for nonprotected Al; the larger reflectance difference at long wavelengths is again explained in terms of surface plasmon excitation. Fig. 4 plots the reflectance of the IBS Al film protected with ED MgF_2, along with the reflectance calculated with the fitting parameters that were obtained in a manner similar to the one described for nonprotected Al in Fig. 2. Reflectance in the NUV is also plotted. The Al roughness parameters of the fitting were σ=3.17 nm and T=30.0 nm. The outer MgF_2 surface was assumed to be smooth; in fact the effect of assigning a roughness to this surface has a much smaller effect on reflectance than at the Al/MgF_2 interface. The presence of MgF_2 has shifted the reflectance loss band to longer wavelengths. This is due to the change in the dielectric constant of the medium from which light impinges on Al, which changes from unity for vacuum to an average of 2.35[31] calculated in the spectral range 140-160 nm. According to Eq. (1), λ_{sp} shifts ideally from 117 to 152 nm. The real wavelength at the peak of reflectance loss depends on the shape of the power spectral density and on the rms roughness, as well as on the metal optical constants. For Al, the wavelength at the reflectance loss peak may be at or somewhat above λ_{sp}[32]. The maximum reflectance

loss in the fitting of Fig. 4 was at 157 nm, whereas that of Fig. 2 was at 127 nm, both in good agreement with the above values obtained from Eq. 1.

Hence, the interpretation of the reflectance loss in terms of surface plasmon excitation given in subsection 3.A is now better understood when we see that the reflectance loss is shifted in the way given by the change of the dielectric constant of the medium from which radiation impinges on Al. The rms roughness is similar in the fittings of Figs. 2 and 4, and the autocorrelation length is now somewhat shorter. Several considerations may explain this shorter value. First, the two samples were obtained in different runs (MgF_2 was not deposited over the same Al sample represented in Fig. 2) and a statistical roughness difference might affect this short-range roughness. Second, roughness is being accounted for through a simple Gaussian function, and the real power spectral density may deviate from this simple function. Finally, the optical constants may deviate from tabulated data (Refs. 23 and 31).

For coatings protected with IBS MgF_2, a reflectance loss similar to the one described above is obtained for the coating with IBS Al compared to ED Al, which can be explained again in terms of surface plasmon excitation. The reflectance at these wavelengths is considerably smaller for the coatings protected with IBS MgF_2 than it was when ED MgF_2 protective coatings were used, due to the larger absorption of the former MgF_2, which was demonstrated in Ref. 19. Hence, at wavelengths longer than ~125 nm two sources of reflectance decay are encountered for coatings prepared all by IBS: surface plasmon excitation due to short-range roughening of IBS Al, and larger absorption of IBS MgF_2.

Fig. 5 extends the reflectance of the four types of coatings at wavelengths up to 850 nm. MgF_2-coated Al, both materials deposited by evaporation, remains the coating with the largest reflectance up to ~350 nm; above this wavelength both types of Al films protected with ED MgF_2 provide a similar reflectance up to 850 nm. The two types of Al coatings protected with IBS MgF_2 exhibit a reflectance close to each other above 220 nm all the way up to 850 nm. The latter coatings reach a reflectance similar to the two coatings protected with ED MgF_2 above ~ 550 nm. From the two factors causing the reflectance loss in the VUV, surface plasmon excitation, which is enhanced with IBS Al films, does not affect reflectance in the visible, whereas the largest absorption of IBS MgF_2 in the VUV propagates to the near UV and the visible, up to the yellow.

Let us suggest lines of improvement on IBS MgF_2 coated Al films. Quesnel et al.[18] deposited IBS MgF_2 by IBS and they used several treatments to improve the films. Their plain IBS MgF_2 samples resulted in a broad absorption band centered at ~260 nm, which still had an enhanced absorption at 800 nm; absorption decreased below the peak, but enhanced absorption was still important at the shortest wavelength investigated (200 nm). The authors explained the absorption peak in terms of the presence of F color centers peaked at 235 nm. The current reflectance data for ED Al protected with IBS MgF_2 show a minimum placed roughly at 200 nm, which suggests that the main source of extra absorption of IBS versus ED MgF_2 is also the presence of F color centers. Quesnel et al.[18] succeeded in reducing IBS MgF_2 absorption first by depositing IBS MgF_2 under a reactive atmosphere with F_2; a second absorption reduction was obtained when they post-treated the samples deposited under reactive atmosphere by annealing at 373 K for several hours, and finally a further absorption decrease was obtained when the samples were cured with UV radiation. The three directions of absorption reduction

might be used to increase the reflectance of IBS MgF_2-protected Al through MgF_2 absorption reduction, which suggests lines of improvement of the coatings investigated in the current research. A temperature of Al film annealing up to 373 K may be compatible with avoiding the growth of larger Al grains, which would be responsible for reflectance decrease through the enhancement of scattering and/or plasmon excitation. Dymshits et al.[33] found that Al films protected with MgF_2, all deposited by ED, can withstand heating up to a temperature of 520 K without permanent degradation in the VUV reflectance. Nonprotected Al films maintained under UHV were also found to withstand annealing at a temperature of 540 K for one hour without any VUV reflectance degradation[34].

Applications of the new coatings are here proposed according to the above results. ED Al protected with IBS MgF_2 is a good choice when the interesting wavelengths are 125 nm and shorter, and also when a large reflectance above 125 nm is not desired because it may mask the range shorter than 125 nm. The hybrid samples deposited in Ref. 19 have similar properties in the short wavelength range to those of the current ED Al coatings protected with IBS MgF_2, although reflectance decay at long wavelengths was smaller in Ref. 19; hence the applicability of the two coatings will depend on the interest on this range. On the other hand, the hybrid samples are more costly than ED Al coatings protected with IBS MgF_2, because the former coatings involve the deposition of an equivalent to 3 materials.

IBS Al protected with ED MgF_2 may find applications, other than for VUV coatings, in the visible. The all IBS-deposited coating may be useful when a high reflectance is required above ~550 nm and sputtering techniques are available better than evaporation

ones. The increased roughness of the Al film may be a problem if, in addition to excite surface plasmons, it also scatters more light. A specific research is suggested towards reducing this roughness with the parameters intrinsic to sputtering, such as ion energy, ion current, and ion species in IBS systems, along with deposition rate and substrate temperature. Suggestions for reducing the absorption of IBS MgF_2 films given in Ref. 18 are considered valuable for the improvement of the current Al coatings protected with IBS MgF_2.

CONCLUSIONS

IBS deposition technique, and this technique combined with evaporation deposition technique are shown to provide valuable coatings of Al protected with MgF_2 both for the VUV and for the visible and near IR.

ED Al film protected with IBS MgF_2 resulted in a reflectance somewhat larger than the standard coating all-deposited by evaporation at wavelengths shorter than 125 nm, whereas the opposite was obtained for wavelengths between 125 and 550 nm. The reflectance of the two types of coatings above 550 nm up to 850 nm was similar.

IBS Al protected with ED and IBS MgF_2 provided a valuable reflectance below 125 nm. IBS Al protected with ED MgF_2 (IBS MgF_2) resulted in a reflectance as large as that of all-evaporated coatings above 350 nm (550 nm). However, IBS Al films were found to have an enhanced surface roughness with large spatial wavevectors that provides a reflectance loss peaked at ~157 nm and extends up to ~350 nm.

ACKNOWLEDGMENTS

This work was supported by the National Programme for Space Research, Subdirección General de Proyectos de Investigación, Ministerio de Ciencia y Tecnología, project numbers ESP2002-01391 and ESP2005-02650. M. Fernández-Perea is thankful to Consejo Superior de Investigaciones Científicas (Spain) for funding under the Programa I3P (Ref. I3P-BPD2004), partially supported by the European Social Fund. We acknowledge the technical assistance of José M. Sánchez Orejuela.

REFERENCES

1. R. P. Madden, L. R. Canfield, G. Hass, "On the vacuum-ultraviolet reflectance of evaporated aluminium before and during oxidation", J. Opt. Soc. Am. **53**, 620-625 (1963)

2. R. C. Vehse, E. T. Arakawa, J. L. Stanford, "Normal-incidence reflectance of aluminum films in the wavelength region 800-2000 Å", J. Opt. Soc. Am. **57**, 551-552 (1967).

3. G. Jezequel, S. Robin, "Propriétés optiques de l'aluminium évaporé en ultravide entre 500 et 1400 Å", Compt. Rend. Acad. Sci. Paris Sér. B **269**, 901-904 (1969).

4. P. H. Berning, G. Hass, R. P. Madden, "Reflectance-increasing coatings for the vacuum ultraviolet and their applications", J. Opt. Soc. Am. **50**, 586-597 (1960).

5. G. Hass, R. Tousey, "Reflecting coatings for the extreme ultraviolet", J. Opt. Soc. Am. **49**, 593-602 (1959).

6. D. W. Angel, W. R. Hunter, R. Tousey, G. Hass, "Extreme ultraviolet reflectance of LiF-coated aluminum mirrors", J. Opt. Soc. Am. **51**, 913-914 (1961)

7. L. R. Canfield, G. Hass, J. E. Waylonis, “Further studies on MgF_2-overcoated aluminium mirrors with highest reflectance in the vacuum ultraviolet”, Appl. Opt. **5**, 45-50 (1966).

8. M. Fernández-Perea, J. A. Aznárez, J. Calvo-Angós, J. I. Larruquert, J. A. Méndez, “Far ultraviolet reflectance variation of MgF2-protected aluminum films under controlled exposure to the main components of the atmosphere”, Thin Solid Films **497** 249-253, (2006)

9. J. B. Kortright, D. L. Windt, “Amorphous silicon carbide coatings for extreme ultraviolet optics”, Appl. Opt. **27**, 2841-2846 (1988).

10. R. A. M. Keski-Kuha, J. F. Osantowski, H. Herzig, J. S. Gum, A. R. Toft, “Normal incidence reflectance of ion beam deposited SiC films in the EUV”, Appl. Opt. **27**, 2815-2816 (1988).

11. G. M. Blumenstock, R. A. M. Keski-Kuha, “Ion-beam-deposited boron carbide coatings for extreme ultraviolet”, Appl. Opt. **33**, 5962-5963 (1994).

12. J. S. Edmends, C. N. Malde´, and S. J. B. Corrigan, ‘‘Measurements of the far ultraviolet reflectivity of evaporated aluminium films under exposure to O_2, H_2O, CO, and CO_2,’’ Vacuum **40,** 471–475 (1990).

13. J. I. Larruquert, J. A. Méndez, J. A. Aznárez, "Far UV reflectance of UHV prepared Al films and its degradation after exposure to O_2", Appl. Opt. **33**, 3518-3522 (1994).

14. T. Kiyota, S. Toyoda, K. Tamagawa, H. Yamakawa, “Aluminum film deposition using an ultrahigh-vacuum sputtering system”, Jpn. J. Appl. Phys. **32**, 930-934 (1993).

15. J. B. Kortright, “Multilayer reflectors for the extreme ultraviolet spectral region”, Nucl. Instr. Meth. Phys. Res. A **246**, 344-347 (1986).

16. L. Martinu, H. Biederman, L. Holland, “Thin films prepared by sputtering MgF_2 in an rf planar magnetron”, Vacuum **35**, 531-535 (1985).

17. T. H. Allen, J. P. Lehan, L. C. McIntyre, Jr, “Ion-beam-sputtered metal fluorides”, in *Optical Thin Films III: New Developments*, R. I. Seddon, Ed., Proc. SPIE **1323**, 277-290 (1990).

18. E. Quesnel, L. Dumas, D. Jacob, F. Peiró, « Optical and microstructural properties of MgF_2 UV coatings grown by ion beam sputtering process”, J. Vac. Sci. Technol. A **18**, 2869-2876 (2000).

19. J. I. Larruquert, R. A. M. Keski-Kuha, “Far ultraviolet optical properties of MgF_2 films deposited by ion-beam sputtering and their application as protective coatings for Al”, Opt. Commun. **215**, 93-99, (2003).

20. J. A. Aznárez, J. I. Larruquert, and J. A. Méndez, “Far-ultraviolet absolute reflectometer for optical constant determination of ultrahigh vacuum prepared thin films”, Rev. Sci. Instrum. **67**, 497-502 (1996).

21. Juan I. Larruquert, José A. Aznárez, José A. Méndez, “FUV reflectometer for in situ characterization of thin films deposited under UHV” in *Instrumentation for UV/ EUV Astronomy and Solar Missions*, Silvano Fineschi, Clarence M. Korendyke, Oswald H. Siegmund, and Bruce E. Woodgate, eds., Proc. SPIE **4139**, 92-101 (2000).

22. S. Tolansky, “Multiple-beam interferometry of surfaces and films”, Oxford University Press, London, 1948.

23. E. Shiles, T. Sasaki, M. Inokuti, D. Y. Smith, “Self-consistency and sum-rule tests in the Kramers-Kronig analysis of optical data: applications to aluminium”, Phys. Rev. B **22**, 1612-1628 (1980).

24. E. D. Palik, "Handbook of optical constants of solids", Academic Press, Orlando, 1985.

25. J. I. Larruquert, J. A. Méndez, J. A. Aznárez, "Far UV reflectance measurements and optical constants of unoxidized Al films", Appl. Opt. **34**, 4892-4899 (1995).

26. J. I. Larruquert, J. A. Méndez, J. A. Aznárez, “Optical constants of aluminum films in the extreme ultraviolet interval of 82-77 nm”, Appl. Opt. **35**, 5692-5697 (1996).

27. G. Hass, J. E. Waylonis, “Optical constants and reflectance and transmittance of evaporated aluminum in the visible and ultraviolet”, J. Opt. Soc. Am. **51**, 719-722 (1961)

28. J. I. Larruquert, J. A. Méndez, J. A. Aznárez, “Degradation of far ultraviolet reflectance of aluminum films exposed to atomic oxygen. In-orbit coating application”, Opt. Comm. **124**, 208-215 (1996)

29. E. Kretschmann, E. Kröger, “Reflection and transmisión of light by a rouge surface, including results for surface-plasmon effects”, J. Opt. Soc. Am. **65**, 150-154 (1975).

30. P. Croce, ‘‘Sur l’effet des couches très minces et des rugosités sur la réflexion, la transmission et la diffusion de la lumière par un dioptre,’’ J. Opt. **8,** 127–139 119772.

31. R. A. M. Keski-Kuha, private communication.

32. J. G. Endriz, and W. E. Spicer, “Study of aluminum films. I. Optical studies of reflectance drops and surface oscillations on controlled-roughness films”, Phys. Rev. B **4**, 4144-4158 (1971).

33. Y. I. Dymshits, V. A. Korobitsyn, A. A. Metel’nikov, „Effect of heating on the reflectivity of aluminum coatings in the vacuum ultraviolet“, Sov. J. Opt. **46**, 649-651 (1979).

34. J. I. Larruquert, J. A. Méndez, J. A. Aznárez, “Non-oxidized Al-overcoated Ir bilayers with high reflectance in the extreme ultraviolet above 50 nm”, Opt. Eng. **41**, 1418-1424 (2002).

FIGURE CAPTIONS

Fig. 1. (Color online) In situ, near-normal reflectance of a nonprotected Al film prepared both by IBS and by evaporation (ED). The calculated reflectance of a smooth Al surface is also displayed

Fig. 2. (Color online) The reflectance of an Al film deposited by IBS and the reflectance calculated with Croce's model with the indicated roughness parameters. The calculated reflectance of a smooth Al surface is also displayed

Fig. 3. (Color online) The reflectance of all combinations of IBS and ED Al protected with MgF_2. Solid line: ED Al. Dashed line: IBS MgF_2. Circles: ED MgF_2. Crosses: IBS MgF_2

Fig. 4. (Color online) The reflectance of an Al film deposited by IBS that was protected with a MgF_2 film deposited by evaporation (ED), and the reflectance calculated with Croce's model with the indicated roughness parameters. The calculated reflectance of a bilayer with smooth surfaces is also displayed

Fig. 5. (Color online) Reflectance of the four types of Al/MgF_2 coatings in the VUV to NIR versus the logarithm of wavelength

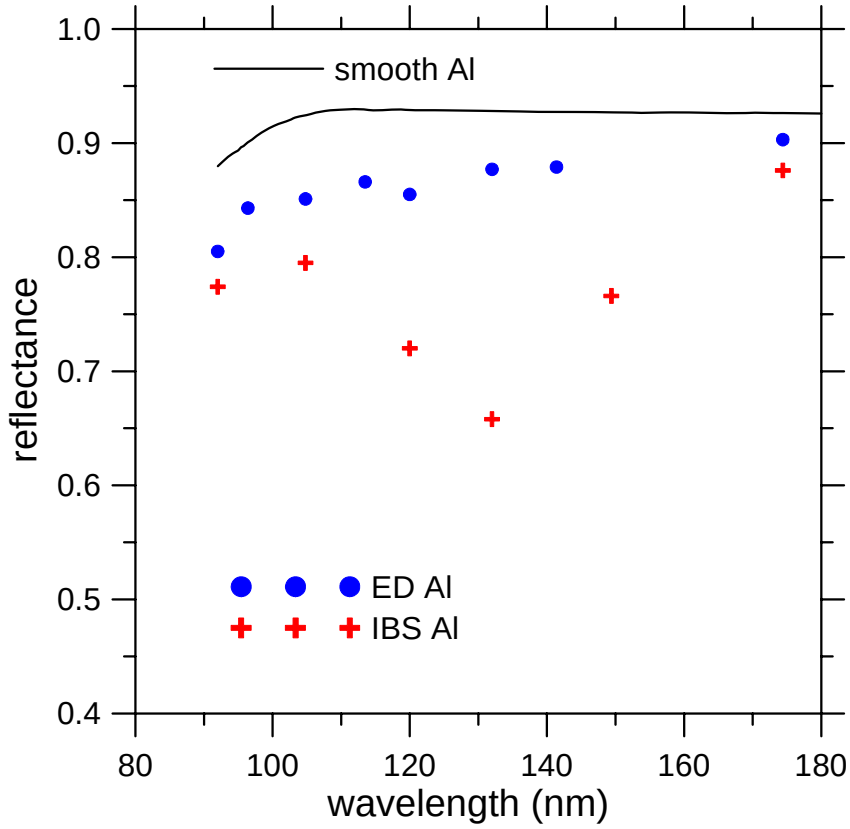
1.0
0.9
0.8
0.7
0.6
0.5
0.4
reflectance
80
100
120
140
160
180
wavelength (nm)
smooth Al
ED Al
IBS Al

Fig. 1

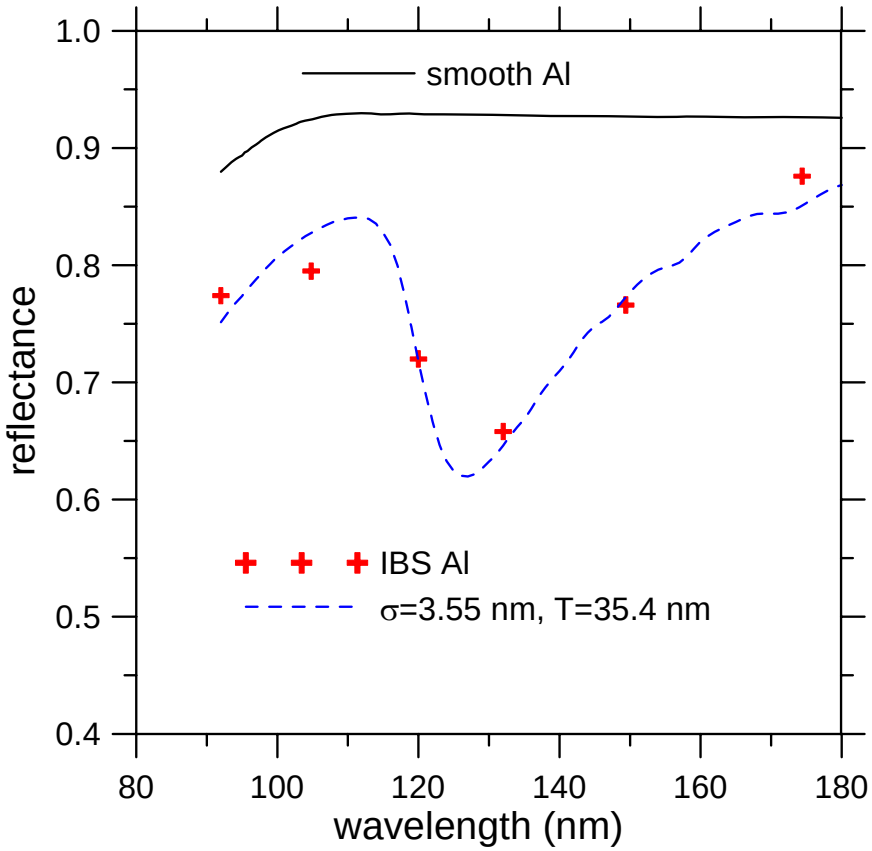
1.0
0.9
0.8
0.7
0.6
0.5
0.4
reflectance
80
100
120
140
160
180
wavelength (nm)
smooth Al
IBS Al
σ=3.55 nm, T=35.4 nm

Fig. 2

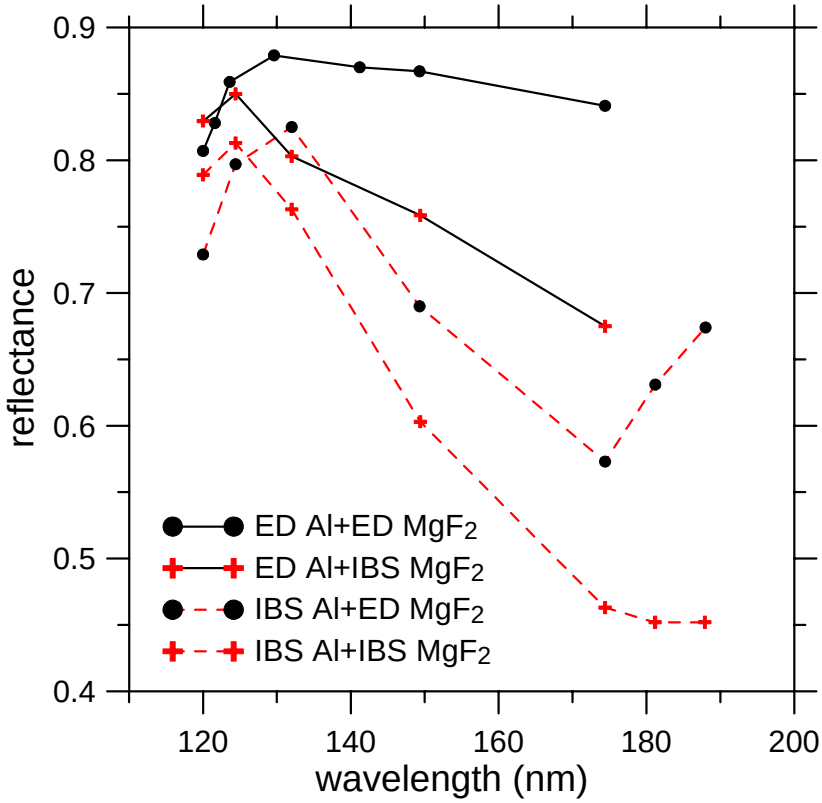
0.9
0.8
0.7
0.6
0.5
0.4
reflectance
120
140
160
180
200
wavelength (nm)
ED Al+ED MgF2
ED Al+IBS MgF2
IBS Al+ED MgF2
IBS Al+IBS MgF2

Fig. 3

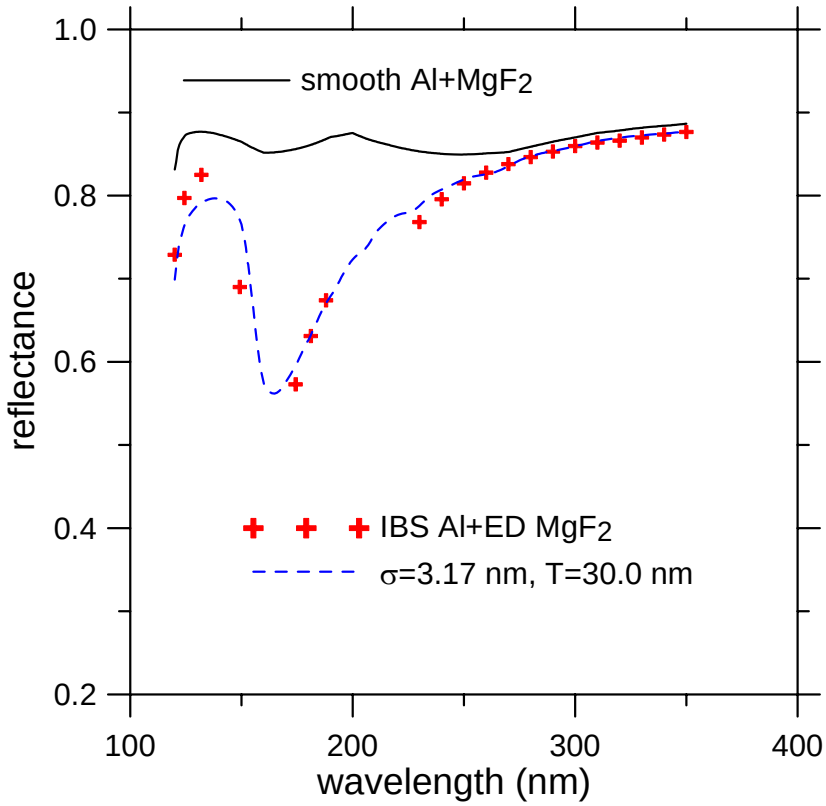
1.0
0.8
0.6
0.4
0.2
reflectance
100
200
300
400
wavelength (nm)
smooth Al+MgF2
IBS Al+ED MgF2
σ=3.17 nm, T=30.0 nm

Fig. 4

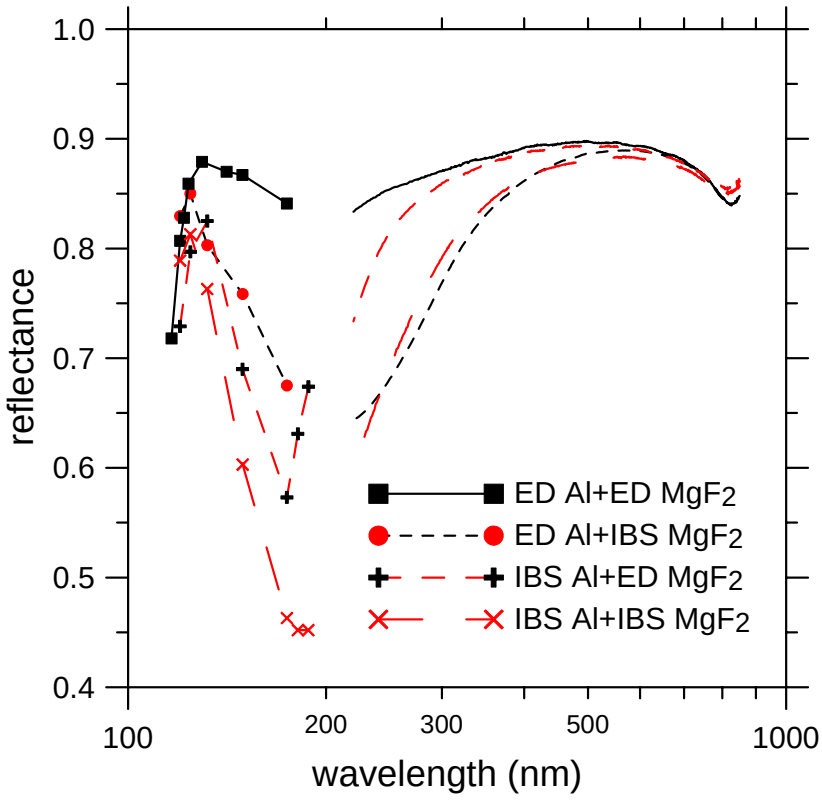
1.0
0.9
0.8
0.7
0.6
0.5
0.4
reflectance
100
200
300
500
1000
wavelength (nm)
ED Al+ED MgF2
ED Al+IBS MgF2
IBS Al+ED MgF2
IBS Al+IBS MgF2

Fig. 5